Contrib Mineral Petrol (2005) 150: 156–173
DOI 10.1007/s00410-005-0009-8

ORIGINAL PAPER

**Else-Ragnhild Neumann · Riccardo Vannucci
Massimo Tiepolo**

N-MORB crust beneath Fuerteventura in the easternmost part of the Canary Islands: evidence from gabbroic xenoliths

Received: 15 February 2005 / Accepted: 19 May 2005 / Published online: 14 July 2005

Abstract Gabbro xenoliths reported in this paper were collected in northern Fuerteventura, the Canary Island located closest to the coast of Africa. The xenoliths are very fresh and consist of Ti–Al-poor clinopyroxene + plagioclase (An_{87-67}) + olivine (Fo_{72-86}) ± orthopyroxene. Clinopyroxene and orthopyroxene are constantly and markedly depleted in light rare earth elements (LREE) relative to heavy REE (HREE), as expected for cumulus minerals formed from highly refractory N-MORB-type melts. In contrast, whole-rock Primordial Mantle-normalized trace element patterns range from mildly S-shaped (mildly depleted in Pr–Sm relative to both the strongly incompatible elements Rb–La and the HREE) to enriched. Estimates show that the trace element compositions of the rocks and their minerals are compatible with formation as N-MORB gabbro cumulates, which have been infiltrated at various extents (≤ 1% to > 5%) by enriched alkali basaltic melts. The enriched material is mainly concentrated along grain boundaries and cracks through mineral grains, suggesting that the infiltration is relatively recent, and is thus associated with the Canary Islands magmatism. Our data contradict the hypothesis that a mantle plume was present in this area during the opening of the Atlantic Ocean. No evidence of continental material that might reflect attenuated continental crust in the area has been found. Gabbro xenoliths with REE and trace element compositions similar to those exhibited by the Fuerteventura gabbros are also found among gabbro xenoliths from the islands of La Palma (western Canary Islands) and Lanzarote. The compositions of the most depleted samples from these islands are closely similar, implying that there was no significant change in chemistry during the early stages of formation of the Atlantic oceanic crust in this area. Strongly depleted gabbros similar to those collected in Fuerteventura have also been retrieved in the MARK area along the central Mid-Atlantic Ridge. The presence of N-MORB oceanic crust beneath Fuerteventura implies that the continent–ocean transition in the Canary Islands area must be relatively sharp, in contrast to the situation both further north along the coast of Morocco, and along the Iberian peninsula.

Communicated by J.L.R. Touret

E.-R. Neumann (✉)
Physics of Geological Processes, University of Oslo, 1048, Blindern, 0316 Oslo, Norway
E-mail: e.r.neumann@geo.uio.no
Tel.: +47-2285-6663
Fax: +47-2285-5101

R. Vannucci
Dipartimento di Scienze della Terra, Università di Pavia, via Ferrata 1, 27100 Pavia, Italy

R. Vannucci · M. Tiepolo
CNR - Istituto di Geoscienze e Georsisorse, sezione di Pavia, Via Ferrata 1, 27100 Pavia, Italy

Introduction

Continental rifting and break-up lead to the formation of different types of passive margins. One type is characterized by extensive extrusive and intrusive magmatism (for example the Vøring and Hatton Bank margins: e.g. Mutter and Zehnder 1988; Morgan et al. 1989; Morgan and Barton 1990). The other main type is non-volcanic margins (examples include the Iberia Abyssal Plain: e.g. Boillot et al. 1989; Whitmarsh and Sawyer 1996; Chian et al. 1999; Skelton and Valley 2000; the conjugate margins east and west of the Labrador Sea: Chian et al. 1995; the margin east of Newfoundland: e.g. Reid 1994; the northern and central Red Sea: e.g. Roeser 1975; Cochran 1983; Bonatti 1985; Martinez and Cochran 1988). Also, among the non-volcanic margins there are differences. Some show a gradual transition from crust and upper mantle with continental characteristics, to lithosphere with oceanic characteristics, expressed in progressive thinning of the continental crust through block rotation and movement along high-angle normal faults, and/or a mixture of continental and oceanic crustal segments (e.g. Pérez-Gussinyé and Reston 2001). The best known examples of transitional ocean-continent margins are the west Iberia margin, where an 80 to 130-km-wide ocean–continent transition zone has been identified (e.g. Boillot and Winterer 1988; Pinheiro et al. 1996; Whitmarsh and Sawyer 1996; Chian et al. 1999), and the northern Red Sea where the whole depression appears to represent stretched continental lithosphere (e.g. Roeser 1975; Cochran 1983; Bonatti 1985; Martinez and Cochran 1988). Other non-volcanic margins show a sharp transition from lithosphere with continental, to lithosphere with oceanic, structure and geophysical characteristic (e.g. the margin east of Newfoundland: Reid 1994). The passive margins along the Atlantic Ocean thus include volcanic as well as both sharp and transitional non-volcanic segments.

So far it is not known why different segments of non-volcanic passive margins develop differently. An important obstacle to further insight and understanding is that our present information on passive margins rests almost exclusively on seismic and density data. An important exception is the west Iberian margin where petrological and geochemical information on crustal and mantle rocks has been made available through several drilling experiments (e.g. Cornen et al. 1996a, b; Seifert and Brunotte 1996; Seifert et al. 1996, 1997). In order to increase our information about, and understanding of, passive margins and their mode of formation, more information on crustal and mantle rocks along different types of passive margins is needed. In some areas, such information may be obtained through the study of mantle and deep crustal xenoliths brought to the surface during volcanic eruptions. The Canary Islands represents such an area. This area is particularly interesting because Ernst and Buchan (1997) and Wilson and Guiraud (1998) have proposed that a mantle plume was located in this area about 200 million years ago, implying that this margin formed as a volcanic rather than a non-volcanic margin. Considerable information about the lithosphere beneath the Canary Islands has already been obtained through studies of mantle and crustal xenoliths from the islands of La Palma, Hierro, Tenerife, and Lanzarote (e.g. Neumann et al. 2000, 2004, and references therein). These studies suggest that the lithosphere beneath large parts of the Canary Islands chain consists of highly refractory N-MORB type oceanic mantle overlain by highly refractory oceanic crust. However, data on xenoliths from the easternmost Canary Island, Fuerteventura (Fig. 1), have not been presented so far. In order to obtain a complete overview of the nature of the continent-ocean transition along the eastern part of the central Atlantic Ocean, it is essential to gain information also on the lower crust beneath the island of Fuerteventura.

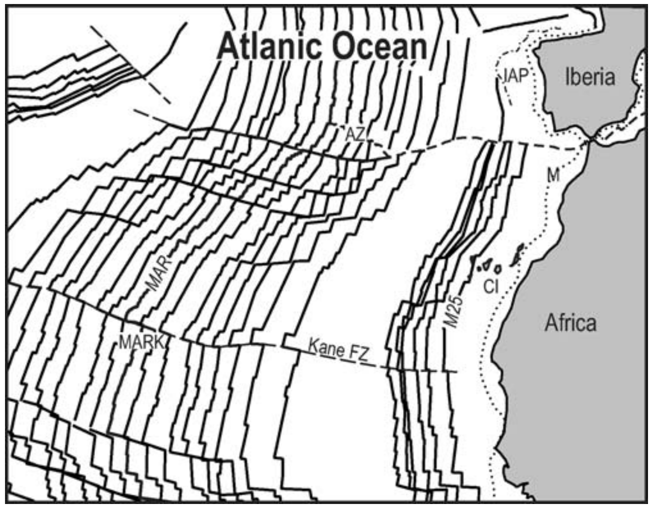

Fig. 1 Map of the east-central Atlantic Ocean with magnetic anomalies from Müller et al. (1997). *AZ* Azores islands, *CI* Canary Islands, *M* Mazagan escarpment, *IAP* Iberia Abyssal Plain, *MAR* mid-Atlantic Ridge, *MARK* mid-Atlantic Ridge south of the Kane Fracture Zone, *dotted line* the edge of the continental platform,; *dash-dot line* the seawards limit of the continent–ocean transition zone outside Iberia

In this paper, data on gabbroic xenoliths from Fuerteventura are presented, including laser ablation (LA) ICP-MS data on pyroxenes. In-situ mineral analyses are eminently suited to "see through" the effects of the Canary Islands event on the old crust on which the islands are built. LA ICP-MS data on gabbroic rocks from the Canary Islands have not been presented before. Together with published data on gabbroic xenoliths from other Canary Islands, the data on the gabbro xenoliths from Fuerteventura are used to discuss (1) the original nature of the passive margin in the area. Because the Canary Islands define a trend normal to the passive margin of the African continent, east–west-related chemical variations in the initial lower crust may be detected through a comparison between gabbroic xenoliths from different islands. We will use available data to discuss also (2) the evolution of the oldest part of oceanic crust in the central Atlantic Ocean. We believe that the petrological and geochemical data presented here provide important information about passive margins, which may be used to gain additional understanding of their different modes of formation.

Geological setting

The Canary Islands are located in the magnetic quiet zone outside Morocco (Figs. 1, 2). The Canary Islands consist of seven large islands that form a roughly east–west trending islands chain located between 100 km and 500 km from the coast of western Africa (Fig. 2). The oceanic lithosphere beneath the Canary Islands formed between ~180 Ma and 190 Ma (easternmost part) and ≈150 Ma ago (westernmost part; e.g. Verhoef et al.

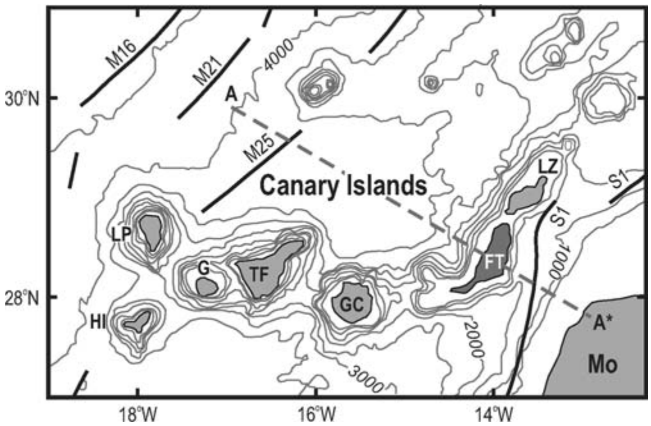

Fig. 2 Map of the Canary Islands showing bathymetry (with 500 m contours) and magnetic anomalies (simplified after Verhoef et al. 1991; Roest et al. 1992; Schmincke et al. 1998). *FT* Fuerteventura, *G* Gomera, *GC* Gran Canaria, *HI* Hierro, *L* Lanzarote, *LP* La Palma, *TF* Tenerife, *Mo* Morocco

1991; Roest et al. 1992; Watts 1994; Hoernle 1998). The Canary Islands formed much later when the Mid-Atlantic Ridge (MAR) was located far west of the Canary Islands. The oldest exposed lavas on the islands show a rough westwards decrease in age from ~24 Ma in Fuerteventura to ~1.1 Ma in Hierro (e.g. Abdel-Monem et al. 1971, 1972; Schmincke 1982; Balogh et al. 1999). However, ages up to 63 Ma obtained on rocks in the basal complex in Fuerteventura (Balogh et al. 1999) suggest that formation of the islands may have started considerably earlier, possibly, ~85 Ma ago (Le Bas et al. 1986). Eruptions in historic times in La Palma, Tenerife, and Lanzarote (e.g. Carracedo and Day 2002) show the Canary hotspot to be still active. Crustal xenoliths have been found in all the large islands.

Fuerteventura is the second largest of the Canary Islands (Fig. 2). An uplifted basal complex is exposed in the western part of the island (e.g. Fúster et al. 1968). The basal complex is dominated by submarine volcanic rocks, but its oldest part consists of large intrusions of ultramafic and mafic rocks and syenites, which are intruded by carbonatites, syenite dykes, and ijolites (e.g. Fúster et al. 1968; Le Bas et al. 1986; Balogh et al. 1999). The youngest parts of the basal complex are made up by gabbros, pyroxenites, basaltic dyke swarms, and syenites (e.g. Stillman et al. 1975; Stillman, 1987; Balogh et al. 1999). The basal complex is overlain by a basaltic shield complex (e.g. Fúster et al. 1968; Coello et al. 1992).

Studies of gabbroic xenoliths from the islands of La Palma, Hierro, Gran Canaria, and Lanzarote suggest that the lower crust beneath most of the Canary Islands consists of a combination of N-MORB-type gabbros that have reacted to different degrees with enriched, alkaline magmas and cumulates formed from alkaline magmas, and gabbroic to syenitic intrusions formed from alkaline magmas (Hoernle 1998; Schmincke et al. 1998; Neumann et al. 2000). A magnetic anomaly, *S*1, is located between the easternmost Canary Islands and Africa (Fig. 1; Verhoef et al. 1991; Roest et al. 1992).

Petrography

The gabbroic xenoliths collected in Fuerteventura are granular with average grain size between 1 mm and 3 mm. The phase assemblage is dominated by plagioclase (ca. 20–60 vol%) and clinopyroxene (ca. 15–40 vol%), with varying proportions of orthopyroxene (not detected to about 40 vol%) and olivine (not detected to about 20 vol%). Minute oxide grains are occasionally present, mainly in glass-fluid inclusion trails (commonly vermicular) and along grain boundaries. Minute grains of apatite have been detected in a few samples by scanning electron microscopy. Like the oxides, apatite is restricted to glass-fluid inclusion trails and grain boundaries. The grains are generally rounded, with interlocking grain boundaries. The best developed convex grain boundaries are generally seen in plagioclase, whereas the other phases partly form rounded grains and partly tend to fill in the spaces between plagioclase grains. Olivine is commonly mildly oxidized. Orthopyroxene is present as separate, rounded grains, as rims on olivine and clinopyroxene, and as exsolution lamellae in clinopyroxene. Clinopyroxene has densely spaced, narrow to wide exsolution lamellae of orthopyroxene; occasionally, the orthopyroxene forms domains in the host clinopyroxene. In some samples, the exsolution lamellae in clinopyroxenes are mildly curved. Unlike orthopyroxene-bearing xenoliths from the other Canary Islands, those from Fuerteventura show no signs of reactions; amphibole has not been observed.

Analytical methods

Major elements in bulk rocks and some trace elements (V, Cr, C, Ni) were determined by X-ray fluorescence spectrometry (XRF) at the Department of Earth Science, University of Bergen, using glass fusion discs and pressed powder tablets and international standards for calibration. Analyses of REE, Li, Rb, Sr, Y, Zr, Nb, Ba, Hf, Ta, Pb, Th, and U were performed by inductively coupled plasma mass spectrometry (ICP-MS) using a Finnigan Element2 housed at the University of Bergen. Approximately 100 mg of rock powder was digested in a mixture of HF, HNO_3, and $HClO_4$ at 200°C. The samples were analyzed in 2% HNO_3 in low- and medium-resolution mode using Indium as an internal standard and the method of standard addition to correct for matrix effects. Accuracy was controlled by measurements of standard samples in each run and normally stayed within ±5%.

Minerals were analyzed for major elements using a CAMECA CAMEBAX Sx100 electron microprobe at the Department of Geology, Oslo University. Accelerating voltage was 15 kV and peaks were counted for 10 s and backgrounds for 5 s. Mafic minerals were analyzed using a beam current of 20 nA and focused beam, whereas plagioclase analyses were performed with a beam current of 10 nA and the beam raster over an area of approximately 10μm×10μm to minimize Na loss. Light elements were counted first to preclude any underestimation. Oxides, natural and synthetic standards have been used. Matrix corrections were performed by the PAP-procedure in the CAMECA software. Analytical precision (2σ error) evaluated by repeated analyses of individual grains is better than ±1% for elements in concentrations of >20 wt% oxide, better than ±2% for elements in the range 10–20 wt% oxide, better than 5% for elements in the range 2–10 wt% oxide, and better than 10% for elements in the range 0.5–2 wt% oxide.

Trace element mineral composition was determined by laser ablation inductively coupled plasma-mass spectrometry (LA ICP-MS) at the CNR-IGG, Pavia. The LA ICP-MS instrument couples a double focussing sector field ICP mass spectrometer (Element IR from ThermoFinnigan) with a Q-switched Nd:YAG laser source (Quantel Brilliant) operating at 213 nm. The laser was operated at a repetition rate of 10 Hz, and the spot diameter was varied from 20 μm to 40 μm with the pulse energy in the range 0.01–0.03 mJ. Helium was used as carrier gas and it was mixed with Ar downstream of the ablation cell. Quantification was done using the NIST SRM 612 glass as the external standard, with ^{44}Ca as internal standard for clinopyroxene and ^{29}Si for orthopyroxene. Precision and accuracy were assessed on the USGS BCR-2(g) reference glass and are both better than 10% for concentration at parts per million level. Full details of the analytical parameters and quantification procedures can be found in Tiepolo et al. (2003).

Whole-rock compositions

Major element compositions and normative minerals (CIPW) of the gabbroic xenoliths from Fuerteventura are given in Table 1. The rocks are silica-saturated (neither normative quartz nor nepheline), MgO concentrations are 8.0–18.7 wt%, and mg# (cation ratio Mg*100/(Mg + Fe_{total})) = 73–86 (Table 1). In general, the concentrations in TiO_2, K_2O and P_2O_5 are low (0.1–0.5 wt% TiO_2; 0.02–0.06 wt% K_2O; ≤ 0.3 wt% P_2O_5); but two samples (FT9-18 and FT9-30A) differ from the others by slightly higher contents of TiO_2 (0.3–1.4 wt%) and K_2O (0.08–0.52 wt%; Fig. 3). High and highly variable Al_2O_3 and CaO concentrations are clearly due to the accumulation of plagioclase and clinopyroxene in different proportions. The compositional characteristics of the gabbro xenoliths are significantly different from those of basaltic lavas, dykes, and gabbroic rocks in the basal complex in Fuerteventura (data by Fúster et al. 1968; Ahijado et al. 2001). This complex mostly contains strongly silica-undersaturated (up to 33% normative nepheline) rocks with high concentrations in TiO_2, K_2O, and P_2O_5. However, a series of roughly silica-saturated dykes is also included. The composition of these dykes is compared with that of gabbro xenoliths in Fig. 3; as a result, the majority of the gabbro xenoliths is strongly depleted in TiO_2, K_2O, and P_2O_5, thus clearly pointing to a different origin.

The gabbro xenoliths from Fuerteventura also show two distinct types of trace element patterns (Table 2; Fig. 4). The majority of the samples have mildly

Table 1 Whole rock major element compositions (wt%) and CIPW norms (wt%) for gabbro xenoliths from Fuerteventura

	FT9-16	FT9-17	FT9-18[a]	FT9-19	FT9-20	FT9-22	FT9-23	FT9-24	FT9-30A[a]	FT9-30B	FT9-31A	FT9-31B
SiO_2	48.97	50.28	47.84	47.40	48.72	48.54	46.29	50.77	47.87	49.53	51.07	50.77
TiO_2	0.17	0.52	0.33	0.19	0.20	0.23	0.12	0.37	0.34	0.10	0.42	0.25
Al_2O_3	15.38	6.18	15.84	15.54	19.47	17.56	13.71	8.98	15.92	20.83	7.56	16.21
$(Fe_2O_3)_{total}$	3.96	9.99	4.38	10.06	5.11	7.98	7.03	7.46	4.89	3.44	10.17	6.70
MnO	0.08	0.21	0.08	0.16	0.10	0.13	0.12	0.17	0.09	0.08	0.21	0.14
MgO	12.38	14.53	14.00	13.28	9.33	10.09	18.71	13.00	13.23	7.97	14.12	9.28
CaO	18.10	16.84	16.64	12.25	15.55	13.98	12.89	17.69	15.96	16.68	15.98	14.65
Na_2O	0.94	0.66	0.89	1.32	1.69	1.60	0.67	0.85	1.02	1.57	0.85	1.76
K_2O	0.03	0.03	0.08	0.03	0.06	0.04	0.02	0.05	0.10	0.04	0.03	0.05
P_2O_5	0.06	0.05	0.06	0.22	0.18	0.12	0.08	0.14	0.16	0.10	0.07	0.14
LOI	0.16	0.15	ND	0.08	0.32	0.26	ND	0.26	0.67	0.69	ND	0.16
Sum	100.23	99.44	100.14	100.53	100.73	100.53	99.64	99.74	100.25	101.03	100.48	100.11
mg#	86.1	74.2	86.4	72.3	78.3	71.5	84.1	77.5	84.3	82.1	73.3	73.3
CIPW norms												
Plag	52.6	17.4	53.3	42.0	61.2	50.1	39.7	26.2	50.4	62.9	19.8	43.1
Cpx	31.8	38.6	26.1	12.3	18.4	15.9	15.3	37.2	22.8	18.2	32.5	18.8
Opx	1.2	36.9	–	30.0	8.1	23.3	19.1	31.4	9.5	12.8	42.0	34.8
Ol	12.3	2.8	18.5	11.7	9.6	7.4	23.3	1.6	14.4	4.4	1.7	0.5
Ilm	0.4	1.1	0.8	0.4	0.5	0.5	0.3	0.8	0.8	0.2	0.8	0.5
Mt	1.5	3.1	1.2	3.0	1.8	2.5	2.2	2.4	1.7	1.1	3.0	2.0
Ap	0.2	0.1	0.2	0.5	0.5	0.3	0.2	0.4	0.4	0.3	0.2	0.3

The norms are calculated assuming $Fe^{2+}/Fe_{total} = 0.85$

LOI loss on ignition, *ND* not detected, mg# cation proportion Mg*100/(Mg + Fe_{total}), *Plag* plagioclase, *Cpx* clinopyroxene, *Opx* orthopyroxene, *Ol* olivine, *Ilm* ilmenite, *Mt* magnetite, *Ap* apatite

[a]Enriched samples

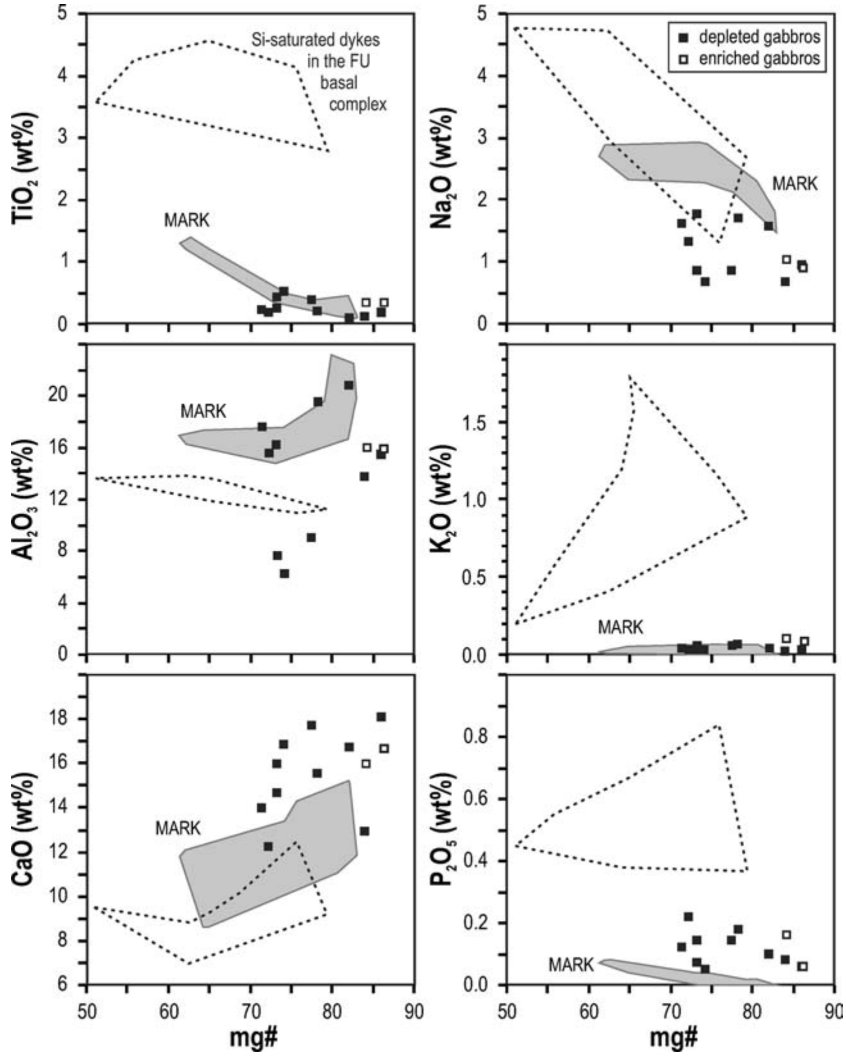

Fig. 3 Major elements in gabbro xenoliths from Fuerteventura plotted against mg# (cation ratio Mg*100/[Mg + Fe_{total}]). The compositions of gabbroic rocks from the MARK area along the MAR (data from Casey 1997), and silica-saturated dykes in the Fuerteventura basal complex (data from Ahijado et al. 2001) are shown for comparison. The figure shows similarity between the Fuerteventura and the MARK gabbros, and none with the strongly Ti–K-enriched dykes in the Basal complex

S-shaped REE patterns (normalized to Primordial Mantle, PM, as defined by McDonough and Sun 1995) with mild depletion in the light and middle REE (LREE and MREE, respectively) relative to the heavy REE (HREE; e.g. $(Nd/Yb)_N = (Nd/Yb)_{sample}/(Nd/Yb)_{PM} = 0.3–0.8$). These samples are referred to below as ‘‘depleted’’. Diagrams showing incompatible trace elements normalized to N-MORB (data from Hofmann 1988) show even more pronounced S-shapes with increasing enrichment factors from the middle REE towards both the most strongly incompatible elements (Rb–Ce), and towards the HREE (Fig. 4). The samples with the most marked Ba- and Sr-peaks and lowest REE contents have the highest proportions of modal and normative plagioclase (e.g. FT9-16: 53% plag; FT9-20: 61% plag; FT9-30B: 63% plag), clearly reflecting accumulation of plagioclase. The lowest Ba- and Sr-anomalies and the highest HREE contents are found in samples with high proportions of clinopyroxene (e.g. FT9-17: 39% cpx; FT9-24: 37% cpx; FT9-31A: 33% cpx), suggesting that in these samples the trace element patterns are strongly influenced by accumulation of clinopyroxene. Similar trace element patterns are exhibited by orthopyroxene-bearing gabbro xenoliths from Lanzarote (Neumann et al. 2000).

The two samples with slightly higher TiO_2- and K_2O-contents (FT9-18 and FT9-30A) are enriched in LREE relative to HREE (e.g. $(Nd/Yb)_N = 2.2–5.1$) (Table 2; Fig. 4) and are referred to below as ‘‘enriched’’.

Mineral chemistry

Olivine

Olivine compositions fall in the range $Fo_{71.6–86.4}$, and 0.11–0.26 wt% NiO, with the exception of sample FT9-31A CaO ≤ 0.1 wt% (Table 3, Fig. 5). The concentration of NiO decreases with decreasing Fo-content, whereas CaO shows no correlation with Fo. Chemical zoning was not observed. The high NiO- and low CaO-contents exhibited by most olivines are typical of abyssal gabbros. In Fig. 5, abyssal gabbros are exemplified by gabbros retrieved from the MARK area along the MAR

Table 2 Trace element compositions (ppm) for gabbro xenoliths from Fuerteventura

	FT9-16	FT9-17	FT9-18[a]	FT9-19	FT9-20	FT9-22	FT9-23	FT9-24	FT9-30A[a]	FT9-30B	FT9-31A	FT9-31B
XRF												
V	121	271	96	123	113	145	87	211	116	101	262	149
Cr	2,000	1,625	1,776	581	650	627	970	2,140	1,413	762	1,430	656
Co	24	57	28	58	27	40	52	41	28	18	55	33
Ni	230	256	335	312	176	197	483	191	374	131	201	132
ICP-MS												
Li	2.62	5.70	3.49	6.37	9.07	4.00	3.12	2.23	4.27	2.00	2.89	4.55
Rb	0.32	0.93	1.45	0.63	0.62	0.28	0.61	0.53	1.59	0.36	0.48	0.58
Sr	50.29	30.90	108.4	88.5	113.4	78.6	58.35	72.4	123.3	79.01	34.61	74.46
Y	4.47	18.62	5.60	6.70	5.65	8.46	3.35	13.28	5.82	3.35	16.74	9.46
Zr	9.69	17.61	21.63	12.41	11.24	8.05	7.92	9.12	23.36	6.04	9.36	10.01
Nb	0.37	0.51	5.11	0.56	0.85	0.21	0.78	0.63	4.83	1.00	0.03	0.97
Ba	11.26	8.47	100.2	22.0	47.33	39.98	34.26	56.13	87.50	41.38	23.58	17.26
Hf	0.35	0.57	0.54	0.40	0.31	0.27	ND	0.29	1.45	ND	0.37	ND
Ta	ND	0.03	0.14	0.05	ND	ND	0.06	ND	0.27	0.07	ND	0.07
Pb	0.75	1.08	0.50	0.75	0.79	0.27	0.47	0.34	2.34	0.51	0.19	0.91
Th	0.07	0.07	0.51	0.78	0.15	0.05	0.09	0.11	0.53	0.12	0.08	0.17
U	0.03	0.05	0.08	0.04	0.05	0.02	0.03	0.05	0.19	0.03	0.02	0.05
La	0.636	0.602	3.997	1.201	1.093	0.509	0.780	0.898	3.665	0.602	0.937	1.900
Ce	1.505	2.062	7.826	3.204	2.527	1.237	1.678	2.066	8.101	1.247	1.858	3.274
Pr	0.220	0.354	1.020	0.408	0.353	0.204	0.236	0.328	1.013	0.171	0.351	0.515
Nd	1.118	2.289	4.277	1.917	1.700	1.214	1.093	1.857	4.321	0.801	2.046	2.479
Sm	0.399	1.269	1.028	0.634	0.575	0.559	0.349	0.884	1.081	0.282	1.005	0.797
Eu	0.168	0.466	0.378	0.326	0.300	0.330	0.173	0.382	0.414	0.172	0.418	0.370
Gd	0.553	2.075	1.020	0.819	0.754	0.894	0.435	1.469	1.083	0.419	1.698	1.129
Tb	0.105	0.417	0.167	0.156	0.136	0.175	0.083	0.284	0.178	0.073	0.343	0.207
Dy	0.719	2.992	0.993	1.045	0.933	1.244	0.551	2.098	1.066	0.531	2.508	1.446
Ho	0.157	0.668	0.195	0.229	0.201	0.280	0.122	0.467	0.212	0.116	0.558	0.320
Er	0.455	1.955	0.539	0.645	0.577	0.814	0.364	1.314	0.585	0.331	1.660	0.936
Tm	0.067	0.294	0.074	0.098	0.085	0.125	0.054	0.199	0.080	0.047	0.254	0.142
Yb	0.433	1.958	0.474	0.662	0.553	0.814	0.355	1.286	0.515	0.308	1.688	0.928
Lu	0.063	0.289	0.066	0.098	0.080	0.118	0.053	0.189	0.076	0.044	0.246	0.137

ND not detected
[a]Enriched samples

(Ross and Elthon 1997; Coogan et al. 2000; Cortesogno et al. 2000). The MARK area is located just south of the Kane Fracture Zone (Fig. 1) and is that part of the MAR, for which chemical data are available, that lies closest to the Canary Islands.

Clinopyroxene

Clinopyroxene is Mg-rich (mg# = 76.5–90.2), has low concentrations in TiO_2 (0.2–0.6 wt%), Al_2O_3 (2.1–3.4 wt%), and Na_2O (0.2–0.5 wt%), but is rich in Cr_2O_3 (0.2–0.7 wt%; Fig. 6; Table 4). There is a weak tendency for decreasing Al and Na from core to rim. Ti is positively, and Al and Cr negatively, correlated with MgO.

In both the "depleted" and the "enriched" samples, the clinopyroxenes are markedly depleted in LREE and other strongly incompatible elements relative to HREE (e.g. $(La/Yb)_N = 0.01–0.09$; Table 5; Fig. 7) and form nearly parallel REE patterns, although two samples (the "depleted" samples FT9-16 and FT9-23) are slightly less depleted in LREE relative to HREE than other samples. The clinopyroxenes in the "enriched" samples have REE patterns similar to those of the most depleted "depleted" xenoliths. There is, however, considerable scatter among the most highly incompatible elements (Rb–Ta). The concentrations in REE, as well as the depletion in Sr relative to LREE, increase with decreasing mg# (Fig. 7). With respect to both major and trace elements clinopyroxene in gabbros from Fuerteventura falls within, or close to, the field defined by clinopyroxene in MARK gabbros. However, although also the elements Rb–Ta fall mostly within the range of MARK gabbros, these elements are less depleted relative to LREE in Fuerteventura gabbros than in those from the MARK area (Fig. 7).

Orthopyroxene

Also, orthopyroxene is Mg-rich (mg#: 71.4–86.7), and has relatively low concentrations in TiO_2 (0.10–0.28 wt%) and Al_2O_3 (1.3–1.6 wt%); CaO-contents are 0.5–1.4 wt% (Table 6; Fig. 8). The concentrations of TiO_2 and CaO increase with decreasing MgO; chemical zoning is negligible. Orthopyroxene in Fuerteventura gabbros is generally more depleted in TiO_2 and CaO than those in MARK gabbros, and tends towards higher MgO and Al_2O_3 concentrations. There are no significant composition differences between orthopyroxene in "depleted" and "enriched" samples.

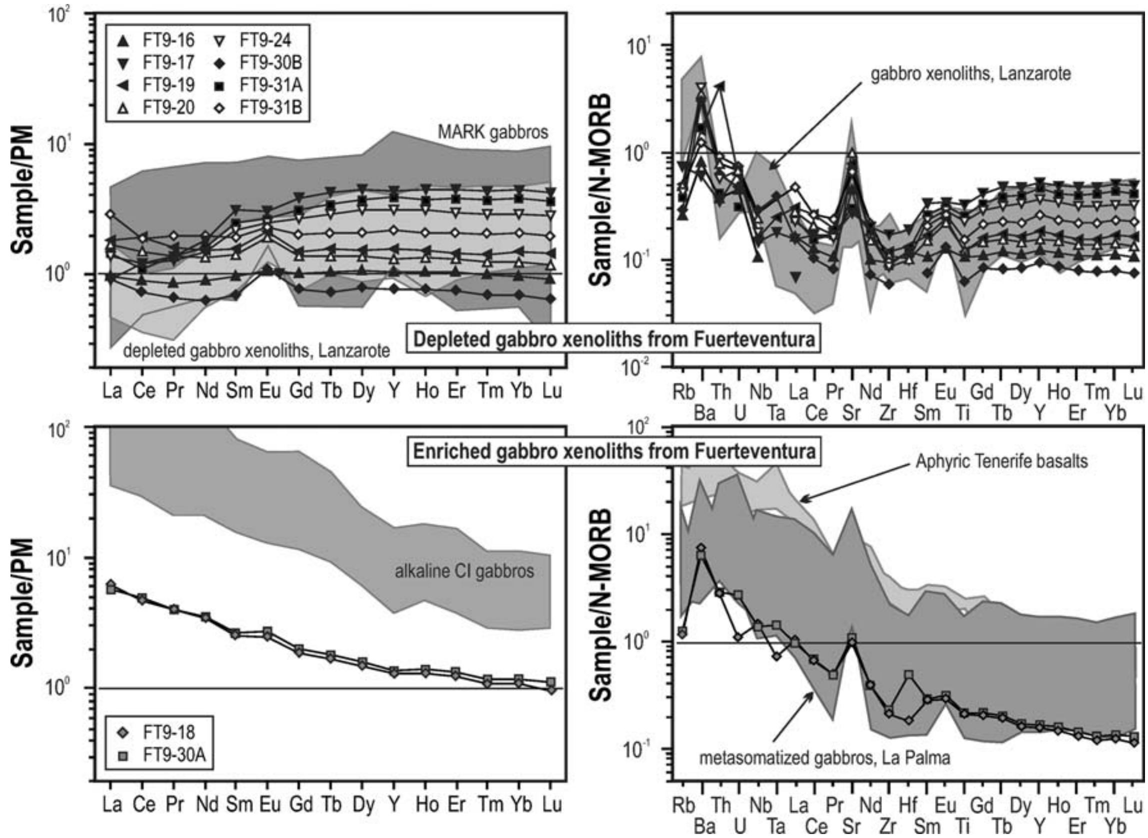

Fig. 4 Rare earth element (REE) and trace element concentrations in selected gabbro xenoliths from Fuerteventura, normalized to primordial mantle (PM; data by McDonough and Sun 1995) and average N-MORB (data by Hofmann 1988), respectively. For comparison are also shown the REE and/or trace element patterns of gabbroic rocks from the MARK area along the MAR (“MARK gabbros”; data from Casey 1997), orthopyroxene-bearing gabbroic xenoliths from Lanzarote (“gabbro xenoliths, Lanzarote”), metasomatized gabbro xenoliths from La Palma (data from Neumann et al. 2000), gabbros from the Canary Islands believed to have formed from alkali basaltic Canary Islands magmas (“alkaline CI gabbros”; data from Neumann et al. 2000), and aphyric basalt lavas from Tenerife (data from Neumann et al. 1999)

The orthopyroxene in three samples were analyzed for trace elements, two “depleted” and one “enriched”. In all three samples, orthopyroxene is strongly depleted in LREE relative to HREE ($(Ce/Yb)_N < 0.01$; Table 7; Fig. 9), although enrichment in the elements Rb–Ta is generally higher than those for LREE.

Plagioclase

Plagioclase compositions fall in the range $An_{87.3}Ab_{12.6}Or_{0.1}$–$An_{67.3}Ab_{32.6}Or_{0.1}$, both normal and reverse zoning is observed (Table 8). An-rich, Or-poor plagioclase, as found in the Fuerteventura gabbros, is typical of N-MORB rocks.

Discussion

The chemical relationships in the gabbro xenoliths from Fuerteventura indicate a two-stage evolutionary history. This is illustrated by (1) the presence of “depleted” as well as “enriched” whole-rock REE patterns (Fig. 4), (2) the S-shaped whole-rock trace element patterns of the “depleted” gabbros, and (3) the presence of clinopyroxene and orthopyroxene with strongly depleted trace

Table 3 Major element compositions (wt%) and forsterite contents (Fo) in olivine in gabbro xenoliths from Fuerteventura

Sample	FT9-16	FT9-18[a]	FT9-20	FT9-22	FT9-23	FT9-30A[a]	TF9-30B	FT9-31A	FT9-31B
SiO_2	39.96	40.24	38.21	36.94	39.59	40.10	38.49	37.97	38.42
FeO	13.91	11.20	21.10	25.81	14.54	13.18	18.29	22.36	22.67
MnO	0.18	0.15	0.33	0.37	0.22	0.20	0.28	0.32	0.38
MgO	46.45	48.16	40.71	36.60	44.28	46.97	42.99	39.44	39.41
NiO	0.20	0.26	0.18	0.14	0.18	0.26	0.19	0.11	0.14
CaO	0.03	0.02	0.03	0.04	0.05	0.02	0.03	0.30	0.00
Sum	100.73	100.06	100.57	99.90	98.85	100.72	100.27	100.50	101.04
Fo	85.6	88.5	77.5	71.6	84.4	86.4	80.7	75.9	84.6

[a]Enriched samples

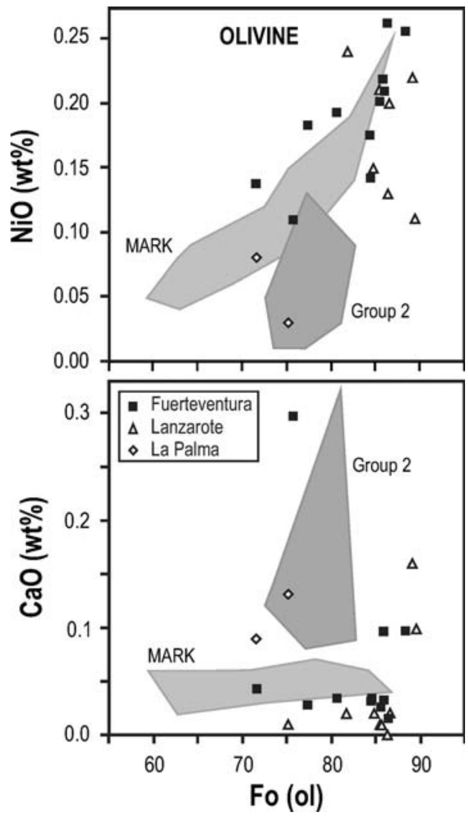

Fig. 5 NiO and CaO plotted against Fo-content in olivine in gabbro xenoliths from Fuerteventura. Olivine in the Fuerteventura gabbros overlap with the mafic part of the field defined by olivine in the MARK area (about 23°N, along the MAR; data from Cannat et al. 1997; Ross and Elthon 1997), whereas olivine in MOR gabbros from the Canary Islands that have reacted with Canary Islands melts (*group 2*; Neumann et al. 2000) have significantly lower contents of NiO, and higher CaO

element patterns in rocks with "enriched" whole-rock pattern (Figs. 7, 9). We show below that the gabbros originally formed from N-MORB melts and were later infiltrated and metasomatized by alkaline melts enriched in strongly incompatible elements.

The original composition of the lower crust beneath Fuerteventura

As shown above, the majority of the gabbros from Fuerteventura ("depleted" xenoliths) shows clear affinity to N-MORB gabbros expressed by low whole-rock concentrations in TiO_2, K_2O, and P_2O_5, and depletion in LREE and MREE relative to HREE (Table. 1, 2; Figs. 3, 4). Also, the low Ti–Al contents and strongly LREE-depleted REE patterns in both clinopyroxene and orthopyroxene are typical of N-MORB gabbros (Tables 4, 5, 6, 7; Figs. 5, 6, 7, 8, 9). The negative correlation between concentrations in incompatible trace elements and mg# exhibited by the pyroxenes clearly reflects formation from melts that have undergone different degrees of fractional crystallization. There are no compositional differences between the minerals from the "enriched" and the "depleted" samples.

We have used the REE concentrations in clinopyroxenes and partition coefficients between clinopyroxene and basaltic melt (using data from Hill et al. 2000, for Ti–Al-poor clinopyroxene) to estimate the REE patterns of the melts that gave rise to the gabbros. The results are shown in Fig. 10. The putative liquids in equilibrium with both the "depleted" and the "enriched" gabbro xenoliths fall below the average N-MORB composition, relative to which they display even a stronger LREE depletion. Basalts with similar REE compositions have been retrieved in the central Red Sea. This implies that the lower crust beneath Fuerteventura initially formed from strongly depleted N-MORB type melts, and that the pyroxenes have essentially retained their original composition.

Available data (e.g. Komor et al. 1990; Niida 1997; Ross and Elthon 1997; Stephens 1997) indicate that the Fo-contents of peridotites collected along the central MAR are concentrated between 90 and 91. Assuming these peridotites to represent residues after formation of N-MORB melts, primary N-MORB melts should be in equilibrium with olivine of composition 90–91. Olivines in the Fuerteventura gabbros have Fo-contents of 71.6–86.4 (Table 3), thus indicating that none of the melts that gave rise to these gabbros were primary, but had all been subjected to some degree of fractional crystallization. The presence of both normal and reverse zoning in some mineral grains (Table 8) suggests that the gabbros formed in magma chambers that were periodically replenished with more mafic magma.

Infiltration/metasomatism

Although both whole-rock and pyroxene data show affinity to N-MORB, the gabbroic xenoliths from Fuerteventura also show features that are not typical of N-MORB gabbros. The S-shaped ("composite") whole-rock trace element patterns of the "depleted" gabbro xenoliths (Fig. 4) imply that the original strongly depleted N-MORB trace element patterns of the gabbros have been superimposed by an enriched pattern, most likely due to infiltration by melts enriched in strongly incompatible relative to mildly incompatible elements. Such infiltration may also explain the mismatch between "enriched" whole-rock REE patterns and depleted pyroxene patterns, as well as the tendency for increasing enrichment factors from MREE to the most strongly incompatible elements exhibited by the pyroxenes (Figs. 7, 9). The shapes of the trace element patterns of the "enriched" Fuerteventura gabbros resemble those of lavas formed from mildly alkaline to transitional Canary Islands melts, and are also exhibited by the Si-saturated dykes in the Fuerteventura basal complex (Fig. 4). However, the concentrations in incompatible elements are significantly lower in the gabbro xenoliths than in the lavas and dykes (Fig. 4).

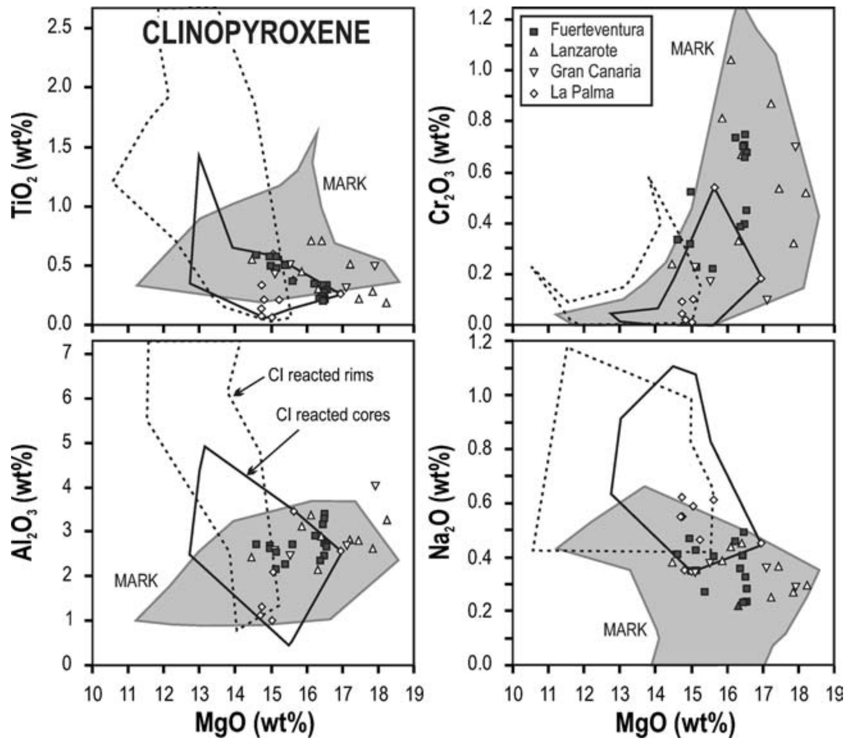

Fig. 6 Major element compositions of clinopyroxenes in gabbro xenoliths from Fuerteventura compared to orthopyroxene-bearing gabbroic rocks from other Canary Islands (data from Schmincke et al. 1998; Neumann et al. 2000), and gabbroic rocks from the MARK area, about 23°N, along the MAR (data from Cannat et al. 1997; Gaggero and Cortesogno 1997; Ross and Elthon 1997; Coogan et al. 2000). Clinopyroxene in gabbroic rocks from the Iberia Abyssal Plain shows significantly higher TiO_2 and Al_2O_3, and lower Cr_2O_3 concentrations (data from Cornen et al. 1996b; Seifert et al. 1997)

As shown above, enrichment in strongly incompatible elements is mainly seen in the whole-rock data (Fig. 4), and appears to have affected the pyroxenes only to a very minor degree (Figs. 7, 9). Apatite (and oxides) is only present as minute grains in glass-fluid inclusion trails and along grain boundaries. This implies that enrichment must be caused by melts that have infiltrated the rocks along grain boundaries and fractures through grains, and that this has happened too recently to allow equilibration between the wall-rock minerals and the infiltrating melts. The infiltrating magmas must consequently belong to the Canary Islands event. It is possible that the infiltration was caused by the lavas that brought xenoliths to the surface.

We tested the suggestion that the trace element patterns of the gabbro xenoliths may be explained by a simple mixing model involving N-MORB cumulates and enriched alkali basaltic magmas. We used the modal proportions of minerals from the norm calculations (Table 1), assuming that olivine, clinopyroxene, orthopyroxene, and plagioclase belong to the original N-MORB gabbro assemblage, whereas oxides and apatite formed from the infiltrating melt. Furthermore, we used the analytical data for clinopyroxene (Table 5), and estimated the trace element compositions of olivine, orthopyroxene, and plagioclase on the basis of clinopyroxene data combined with two-mineral and mineral/melt partition coefficients (namely olivine/clinopyrox-

Table 4 Major element compositions in clinopyroxene (wt%) in gabbro xenoliths from Fuerteventura. Open spaces mean not analyzed

Sample	FT9-16			FT9-17	FT9-18[a]	FT9-20	FT9-22		FT9-23	FT9-24	FT9-30A[a]		TF9-30B		FT9-31A	FT9-31B
Comment	Large		Small													
	Core	Rim					Core	Rim			Core	Rim	Core	Rim		
SiO_2	52.16	52.41	52.48	50.54	51.70	51.15	50.87	51.18	52.27	51.32	52.24	52.66	51.75	51.95	50.68	52.24
TiO_2	0.24	0.33	0.35	0.58	0.21	0.36	0.58	0.50	0.34	0.49	0.27	0.29	0.20	0.22	0.57	0.47
Al_2O_3	3.14	2.74	2.89	2.72	3.70	2.69	2.54	2.26	2.65	2.63	3.29	2.70	2.46	2.34	2.67	2.14
Cr_2O_3	0.70	0.70	0.73	0.33	0.75	0.22			0.45	0.52	0.66	0.67	0.40	0.38	0.32	0.22
FeO	3.54	3.56	3.51	7.47	3.20	5.68	7.04	6.87	3.75	5.99	3.56	3.35	5.05	4.81	8.22	6.88
MnO	0.11	0.11	0.11	0.20	0.11	0.17	0.20	0.20	0.14	0.16	0.13	0.13	0.14	0.15	0.20	0.21
MgO	16.45	16.48	16.25	14.62	16.52	15.62	15.16	15.40	16.58	14.99	16.52	16.57	16.49	16.38	14.98	15.17
NiO	0.04	0.05	0.03	0.02	0.04	0.04	0.04	0.04	0.10	0.01	0.03	0.02	0.05	0.03	0.04	0.02
CaO	23.92	24.27	23.42	22.11	23.72	22.75	22.15	22.34	22.54	22.49	23.98	24.53	22.58	23.02	21.52	22.85
Na_2O	0.40	0.23	0.46	0.41	0.23	0.40	0.42	0.27	0.28	0.35	0.33	0.24	0.49	0.36	0.47	0.35
Sum	100.70	100.88	100.22	99.01	99.87	98.89	98.99	99.05	99.07	98.95	101.00	101.15	99.61	99.65	99.66	100.56

[a]Enriched samples

Table 5 Trace element compositions (ppm) in clinopyroxene in gabbro xenoliths from Fuerteventura (with 1σ analytical error)

Sample	FT9-16		FT9-17		FT9-18[a]		FT9-20		FT9-22		FT9-23		FT9-24		FT9-30A[a]		FT9-31A		FT9-31B	
n	3	1σ Error	4	1σ Error	4	1σ Error	3	1σ Error	4	1σ Error	4	1σ Error	4	1σ Error	4	1σ Error	5	1σ Error	2	1σ Error
Li	0.28	0.08	2.38	0.38	2.52	0.63	0.96	0.15	< 0.7		< 1.3		< 0.8		1.34	0.22	1.00	0.11	3.63	0.49
Sc	87	14	121	4	95	3	123	28	110	4	105	4	122	4	93	16	120	13	90	3
Ti	1,320	190	4,390	280	1,540	70	2,870	790	3,820	210	1,580	80	3,400	270	1,500	230	4,240	540	2,820	130
V	290	50	550	20	277	9	490	100	470	20	330	10	450	20	290	60	490	50	330	10
Cr	5,600	1,200	3,170	240	6,900	600	3,930	190	3,200	220	5,700	590	3,970	360	2,360	560	2,430	90	1,460	110
Co	40.9	6.2	69.9	5.2	40.2	2.6	60.0	2.2	52.4	3.4	47.4	3.6	59.6	5.5	38.8	6.6	62.3	2.0	88.0	4.2
Rb	0.034	0.012	< 0.16		< 0.17		< 0.08	0.034	< 0.15		< 0.19		< 0.14		0.038	0.014	0.057	0.033	< 0.15	
Sr	4.14	0.27	5.22	0.31	5.74	0.328	5.05	0.78	3.91	0.21	4.03	0.27	5.05	0.37	3.51	0.24	4.10	0.31	1.80	0.10
Y	6.5	0.5	23.2	1.2	6.3	0.5	14.8	2.9	22.3	1.0	9.6	0.8	17.0	1.0	8.0	0.6	17.7	1.6	11.0	0.7
Zr	8.28	0.75	9.65	0.72	3.07	0.21	12.0	0.8	13.5	0.9	8.66	0.67	5.64	0.52	2.06	0.19	7.08	0.30	4.98	0.29
Nb	0.071	0.009	0.147	0.013	0.0168	0.005	0.084	0.007	0.069	0.007	0.1053	0.013	0.030	0.004	0.0301	0.0027	0.0137	0.0028	0.040	0.006
Cs	< 0.009		< 0.06		< 0.06		< 0.023		< 0.06		< 0.07		< 0.05		< .01		< 0.015		< 0.06	
Ba	< 0.03		0.07	0.02	< 0.04		< 0.07		< 0.06		0.041	0.017	< 0.5		0.066	0.013	0.211	0.023	0.10	0.02
La	0.110	0.008	0.138	0.009	0.052	0.005	0.135	0.020	0.178	0.010	0.102	0.007	0.091	0.007	0.018	0.002	0.109	0.009	0.108	0.004
Ce	0.579	0.031	1.045	0.065	0.316	0.015	1.06	0.11	1.356	0.075	0.486	0.023	0.636	0.048	0.214	0.012	0.713	0.038	0.390	0.017
Pr	0.128	0.014	0.298	0.014	0.105	0.007	0.294	0.033	0.375	0.017	0.139	0.009	0.178	0.010	0.081	0.009	0.216	0.013	0.162	0.009
Nd	0.88	0.11	2.6	0.1	0.84	0.07	2.29	0.26	2.88	0.11	1.01	0.10	1.71	0.07	0.74	0.10	1.90	0.11	0.99	0.07
SM	0.452	0.068	1.457	0.071	0.523	0.062	1.36	0.12	1.72	0.08	0.623	0.086	1.182	0.064	0.461	0.073	1.230	0.062	0.617	0.064
Eu	0.176	0.024	0.546	0.029	0.220	0.027	0.467	0.024	0.597	0.030	0.249	0.037	0.416	0.026	0.217	0.031	0.480	0.019	0.278	0.029
Gd	0.747	0.088	2.73	0.15	0.951	0.065	2.15	0.12	2.67	0.14	1.198	0.086	2.10	0.13	0.90	0.12	2.27	0.09	1.28	0.08
Tb	0.152	0.013	0.556	0.028	0.169	0.010	0.412	0.033	0.546	0.026	0.229	0.014	0.403	0.023	0.194	0.018	0.442	0.021	0.279	0.014
Dy	1.265	0.062	4.17	0.25	1.31	0.07	3.18	0.57	4.24	0.23	1.71	0.10	3.22	0.23	1.476	0.075	3.46	0.30	2.13	0.10
Ho	0.267	0.017	0.931	0.059	0.305	0.019	0.676	0.023	0.950	0.053	0.421	0.029	0.720	0.055	0.326	0.022	0.753	0.024	0.484	0.026
Er	0.765	0.047	2.82	0.18	0.861	0.056	2.33	0.14	3.02	0.17	1.304	0.092	2.16	0.17	0.98	0.06	2.33	0.09	1.57	0.09
Tm	0.111	0.012	0.422	0.027	0.129	0.009	0.331	0.069	0.419	0.025	0.191	0.014	0.324	0.025	0.144	0.016	0.340	0.034	0.245	0.014
Yb	0.835	0.055	2.90	0.15	0.89	0.07	2.18	0.36	2.84	0.14	1.35	0.12	2.24	0.14	1.07	0.07	2.43	0.20	1.89	0.12
Lu	0.128	0.007	0.419	0.021	0.123	0.010	0.385	0.061	0.398	0.019	0.195	0.017	0.316	0.019	0.151	0.009	0.346	0.027	0.261	0.016
Hf	0.215	0.012	0.558	0.031	0.181	0.016	0.39	0.09	0.543	0.031	0.278	0.021	0.316	0.021	0.142	0.008	0.399	0.043	0.257	0.017
Ta	0.0043	0.0011	0.0030	0.0014	0.0050	0.0015	0.023	0.003	0.013	0.002	0.028	0.003	0.006	0.001	0.0045	0.0007	< 0.003		0.005	0.001
Pb	0.0185	0.0035	< 0.03		< 0.03		< 0.02		< 0.03		0.069	0.014	< 0.03		0.0220	0.0037	0.318	0.018	< 0.03	
Th	0.0050	0.0007	0.0031	0.0007	0.0042	0.0009	0.006	0.002	0.012	0.002	0.0054	0.0010	0.0006	0.0003	0.0114	0.0011	0.0016	0.0004	0.0217	0.0022
U	0.0031	0.0005	0.0037	0.0007	0.0010	0.001	0.0029	0.0010	0.010	0.001	0.0060	0.0008	0.0019	0.0005	0.0025	0.0001	0.0008	0.0003	0.0033	0.0008

N number of samples
[a]Enriched samples

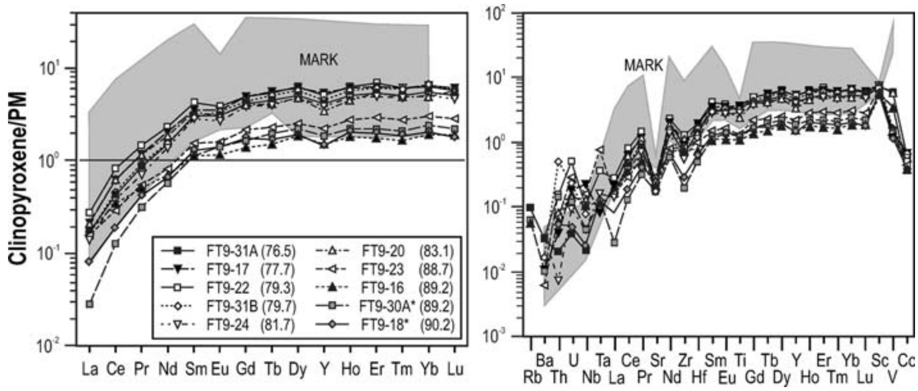

Fig. 7 REE and spider diagrams for clinopyroxenes in gabbro xenoliths from Fuerteventura, normalized to PM (McDonough and Sun 1995). Mg#-numbers are given in parentheses. The *gray field* represents clinopyroxene in gabbroic rocks from the MARK area along the MAR (data from Ross and Elthon 1997; Coogan et al. 2000; Cortesogno et al. 2000). Sample names ending with *asterisks* indicate "enriched" samples

ene, orthopyroxene/clinopyroxene, clinopyroxene/melt, and plagioclase/melt) for tholeiitic systems; the trace element compositions of apatite and magnetite have been calculated from apatite/melt and magnetite/melt partition coefficients for alkali basaltic systems (Table 9). As model for the infiltrating melt we have used the composition of an alkali basaltic dyke (TF20) in Tenerife.

Assuming a very low proportion of trapped melt, we were able to reproduce quite well the S-shaped trace element patterns of the "depleted" samples, as well as the different degrees of positive anomalies for Ba and Sr. In Fig. 11, we show the results for 0.8% trapped melt in all the "depleted" samples. For the "enriched" samples FT9-18 and FT9-30A, we obtained a relatively good fit between observed and estimated trace element patterns, assuming 5% of trapped melt in addition to crystallization of Fe–Ti oxides and apatite from the infiltrating melt (Fig. 11).

Some deviations between estimated and observed trace element concentrations (e.g. Nb, Ta, and Zr among the "depleted" samples) may be related to either the assumption that all infiltrated melts had the same composition and/or to the choice of inaccurate partition coefficients. Furthermore, the melt-rock mixing model proposed here is clearly an oversimplification of the real infiltration process, which probably also involves some chemical exchange between the infiltrating melt and the wall-rock minerals. This is verified by the higher-than-expected and highly variable concentrations in the most strongly incompatible elements in both clinopyroxene and orthopyroxene (Figs. 7, 9). In spite of the deviations between observed and estimated trace element concentrations, we conclude that the gabbros represent N-MORB cumulates which have been infiltrated to different degrees by enriched alkali basaltic magmas belonging to the Canary Islands magmatism. The only difference between the "enriched" and the "depleted" samples appears to be a significantly more extensive degree of infiltration in the "enriched", than in the "depleted", gabbros.

Gabbro xenoliths from Fuerteventura compared to ones from the other Canary Islands

Rare earth elements and trace element compositions similar to those exhibited by the Fuerteventura gabbros are also found among gabbro xenoliths from La Palma, Gran Canaria, and Lanzarote (Schmincke et al. 1998; Neumann et al. 2000). The compositions of the "depleted" samples closely resemble those of orthopyroxene-bearing gabbro xenoliths from Lanzarote, whereas the "enriched" samples resemble gabbro xenoliths from

Table 6 Major element compositions (wt%) in orthopyroxene in gabbro xenoliths from Fuerteventura. Open spaces mean not analyzed

Sample	FT9-16	FT9-17	FT9-20		FT9-22		FT9-30A[a]	TF9-30B		FT9-31A	FT9-31B
			Core	Rim	Core	Rim		Core	Rim		
SiO_2	55.82	53.19	53.97	53.93	53.01	53.16	56.32	54.49	54.19	52.27	53.97
TiO_2	0.12	0.28	0.23	0.23	0.25	0.21	0.11	0.12	0.10	0.28	0.21
Al_2O_3	1.31	1.54	1.56	1.59	1.28	1.23	1.59	1.64	1.59	1.54	1.27
Cr_2O_3	0.15	0.17			0.32	0.33	0.18	0.21	0.18	0.17	0.15
FeO	9.10	16.82	13.57	13.43	16.16	16.25	8.98	12.11	12.19	18.08	17.71
MnO	0.23	0.36	0.33	0.33	0.38	0.38	0.22	0.30	0.28	0.40	0.41
MgO	32.57	26.18	29.28	29.20	27.14	27.21	32.82	30.21	30.37	25.37	26.27
NiO	0.04	0.04	0.06	0.05	0.02	0.03	0.06	0.05	0.04	0.05	0.04
CaO	0.45	1.12	0.61	0.93	1.07	0.95	0.65	0.98	0.73	1.44	0.95
Na_2O	0.04	0.03	0.06	0.01	0.01	0.03	0.09	0.08	0.09	0.11	0.01
SUM	99.82	99.74	99.67	99.70	99.33	99.45	101.17	100.21	99.77	99.70	100.98

[a]Enriched samples

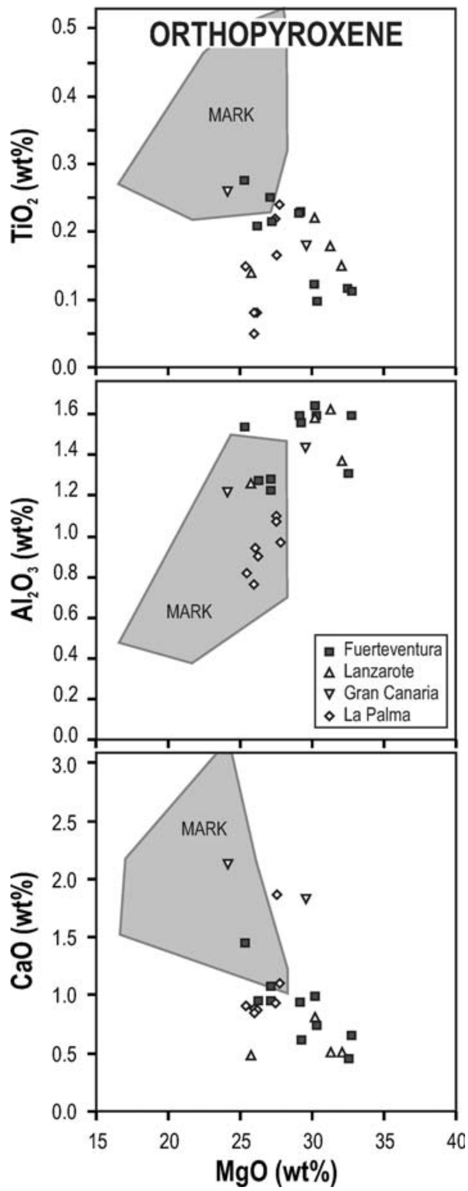

Fig. 8 Ti–Al–Ca–mg# relationships in orthopyroxene in gabbro xenoliths from Fuerteventura compared to orthopyroxene in gabbroic rocks from Lanzarote, Gran Canaria, and La Palma, believed to have formed from N-MORB melts (Schmincke et al. 1998; Neumann et al. 2000), and orthopyroxene in gabbroic rocks from the MARK area (Cannat et al. 1997; Ross and Elthon 1997). The lower CaO-contents in orthopyroxene in gabbroic rocks in the Canary Islands than in the MARK area most likely reflect equilibration to lower temperatures of the old oceanic crust beneath the Canary Islands. The highly LREE-depleted clinopyroxenes from Fuerteventura show a striking similarity to those in MARK gabbroic rocks

La Palma which show evidence of reactions, including formation of amphibole at the expense of clinopyroxene (Neumann et al. 2000; Fig. 9). Also, these xenoliths were interpreted as N-MORB gabbros which have been mildly to strongly infiltrated by enriched Canary Islands magmas (Neumann et al. 2000). Ar–Ar age determinations on plagioclase and hornblende in tholeiitic gabbro

Table 7 Trace element compositions (ppm) in orthopyroxene in gabbro xenoliths from Fuerteventura (with 1σ analytical error)

Sample	FT9-20		FT9-30A[a]		FT9-31A	
n	2	1σ	4	1σ	5	1σ
Li	0.80	0.11	1.97	0.37	0.81	0.09
Sc	31.3	4.7	24.9	4.8	37.6	2.9
Ti	1,380	250	530	120	1,540	140
V	145	14	103	23	160	9
Cr	776	75	1,040	230	991	56
Co	85.6	8.0	77	20	84.7	4.6
Rb	< 0.07		0.048	0.011	< 0.04	
Sr	0.780	0.067	0.0122	0.0068	0.061	0.012
Y	1.25	0.22	0.63	0.13	2.22	0.20
Zr	0.699	0.049	0.070	0.01	0.523	0.0317
Nb	0.0117	0.0032	0.0248	0.0046	< 0.06	
Cs	< 0.016		< 0.007		< 0.013	
Ba	0.318	0.026	0.103	0.017	0.094	0.017
La	< 0.006		< 0.0024		< 0.005	
Ce	< 0.014		0.0037	0.0009	0.0103	0.0021
Pr	0.0036	0.0013	< 0.001		0.0037	0.0010
Nd	0.0302	0.0046	0.0090	0.0029	0.0396	0.0059
Sm	0.0098	0.0027	0.0052	0.0017	0.0301	0.0053
Eu	0.0114	0.0020	0.00238	0.00084	0.0154	0.0019
Gd	0.054	0.017	0.0204	0.0074	0.099	0.016
Tb	0.0131	0.0018	0.0063	0.0014	0.032	0.002
Dy	0.157	0.020	0.082	0.017	0.317	0.022
Ho	0.0472	0.0049	0.0259	0.0057	0.0939	0.0054
Er	0.220	0.027	0.097	0.022	0.393	0.026
Tm	0.0441	0.0088	0.0190	0.0047	0.075	0.008
Yb	0.434	0.079	0.186	0.042	0.65	0.06
Lu	0.0737	0.0078	0.0320	0.0065	0.115	0.0069
Hf	0.0272	0.0065	0.0115	0.0024	0.0406	0.0048
Ta	< 0.007		0.00178	0.00052	< 0.003	
Pb	< 0.007		0.0270	0.0059	0.389	0.034
Th	0.00113	0.00039	0.00094	0.00029	< 0.0004	
U	< 0.0009		0.00035	0.00009	< 0.0005	

n number of analyses
[a]Enriched sample

xenoliths from Gran Canaria giving ages of 164 ± 3 to 178 ± 17 Ma support the conclusions that the tholeiitic gabbros from the different Canary Islands represent the oceanic crust formed during the opening of the central Atlantic Ocean (Schmincke et al. 1998).

In order to compare the original composition of different part of the oceanic crust beneath the Canary Islands, it is necessary to "see through" the effects of the Canarian intraplate event. It is clear from a comparison between trace element data on minerals and rocks (Figs. 4, 7, 9) that metasomatism and reactions with Canarian magmas have affected the most highly incompatible elements more than the moderately incompatible ones. Shervais (1982) has shown that, like REE, the Ti–V relationships are diagnostic of tectonic setting, and may also be used to separate rock series within the same area. In Fig. 12, we compare the V–TiO_2 relationships in gabbroic xenoliths from different Canary Islands. Orthopyroxene-bearing gabbroic rocks of *group 1* (N-MORB gabbros very mildly affected or unaffected by the Canarian magmatism) from La Palma, Lanzarote, and Fuerteventura show uniform, low Ti/V ratios (6–10). *Group 2* samples (N-MORB gabbros

Table 8 Major element compositions and An–Ab–Or relationships in plagioclase in gabbro xenoliths from Fuerteventura. I and II represents typical compositions of two different groups of plagioclase

Sample	FT9-16		FT9-20		FT9-22				FT9-24		FT9-30A[a]		FT9-31B	
Comment	Core	Rim	Core	Rim	Core I	Rim I	Core II	Rim II	Core	Rim	Core I	Core II	Core	Rim
SiO_2	46.62	46.02	48.74	49.63	46.44	46.23	48.65	50.51	49.74	49.38	46.63	46.08	51.55	49.19
Al_2O_3	32.86	33.23	31.73	31.56	32.41	33.01	31.68	30.58	30.66	30.79	33.02	32.35	30.07	31.97
Fe_2O_3	0.17	0.15	0.38	0.38	0.27	0.29	0.38	0.34	0.35	0.28	0.27	0.26	0.28	0.27
CaO	17.66	17.98	16.05	15.32	17.09	17.38	16.14	14.44	14.86	15.24	17.81	17.50	13.95	15.86
Na_2O	1.70	1.44	2.62	3.00	1.77	1.50	2.56	3.47	3.17	2.95	1.68	1.97	3.74	2.63
K_2O	0.01	0.01	0.01	0.01	0.01	0.02	0.02	0.02	0.02	0.03	ND	ND	0.02	0.03
Sum	99.04	98.83	99.52	99.89	97.99	98.43	99.43	99.37	98.80	98.66	99.41	98.15	99.60	99.96
An	85.1	87.3	77.2	73.8	84.2	86.4	77.6	69.6	72.1	74.0	85.5	83.1	67.3	76.8
Ab	14.8	12.6	22.8	26.1	15.8	13.5	22.3	30.3	27.8	25.9	14.5	16.9	32.6	23.0
Or	0.1	0.1	0.1	0.1	0.1	0.1	0.1	0.1	0.1	0.1	<0.1	<0.1	0.1	0.2

An anorthite, *Ab* albite, *Or* orthoclase, *ND* not detected
[a]Enriched samples

moderately to strongly infiltrated by Canarian magmas) tend towards somewhat higher ratios (mainly between 10 and 22), whereas *group 3* gabbros (formed from enriched Canarian magmas) show significantly higher ratios (50 to ≥150), overlapping with Canary Islands lavas. Melts of similar REE compositions as those estimated for the lower crust beneath the Canary Islands, and similar Ti/V ratios, appear also to have given rise to some of the very young gabbroic rocks in the MARK area (Casey 1997).

The low, uniform Ti/V ratios in *group 1* gabbros from the different Canary Islands (Fig. 12) indicate a uniform degree of depletion from east to west in the old oceanic crust beneath the Canary Islands. This is taken to imply that there was no significant change in degree of partial melting or mantle source composition during the first ca. 30 Ma (ca. 180–150 Ma) of the opening of the central Atlantic Ocean in this area. The low, uniform Ti/V ratios also imply that involvement of the continental crust is negligible.

Implications

Ernst and Buchan (1997) and Wilson and Guiraud (1998) proposed that a mantle plume was located below western Africa about 200 million years ago, and that this plume is reflected in the chemical characteristics of the oldest seafloor in the central Atlantic Ocean. This hypothesis has been debated. Janney and Castillo (2001) have presented evidence that the oldest basalts (160–120 Ma) sampled by deep-sea drilling from the central Atlantic oceanic crust have isotopic and chemical signatures compatible with plume contamination. Most of the samples included in this study were collected in the western Atlantic Ocean; only one sample was located in the eastern Atlantic, close to the M23 magnetic anomaly southeast of Cape Verde. McHone (2000), in contrast, claims that the Early Jurrassic magmatism that accompanied the opening of the central North Atlantic Ocean occurs in overlapping provinces of distinct dyke trends and compositional types, not as magmas associated with a single plume, Furthermore, according to McHone (2000) there are no hotspot tracks in the central Atlantic crust that may have been generated by a ca. 200 Ma year old plume. Magmatism associated with mantle plumes (OIB) differs significantly from N-MORB magmas for its generally enriched (or not depleted) PM-normalized incompatibility diagrams (LREE/HREE≥ 1.0 and Ti/V> >10; e.g. Schilling 1973; Schilling et al. 1983; Sun and McDonough 1989; Casey 1997; Hannigan et al. 2001). The data on *group 1* gabbros (Figs. 4, 5, 6, 7, 8, 9,

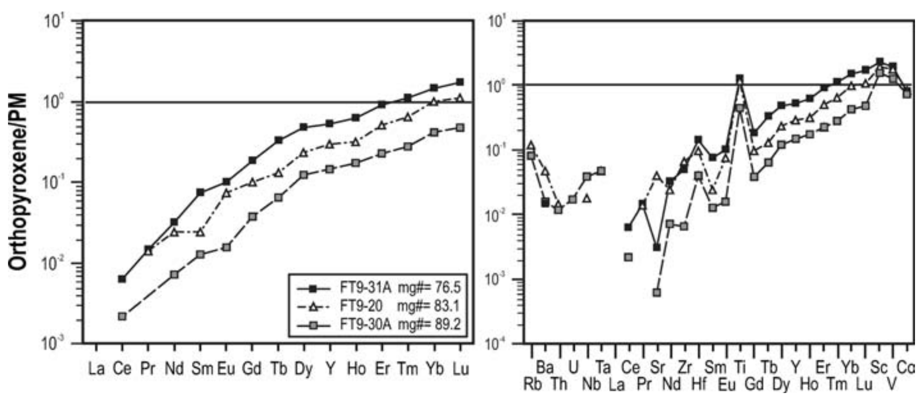

Fig. 9 REE and spider diagrams for orthopyroxene in gabbro xenoliths from Fuerteventura normalized to PM as given by McDonough and Sun (1995). The orthopyroxenes are strongly depleted in LREE relative to HREE, but exhibit higher enrichment factors for the elements Rb–Ta than for LREE. Samples names ending with *asterisks* indicate "enriched" samples

Table 9 Mineral/mineral and mineral/melt partition coefficients with references used to estimate the trace element compositions of the melts that gave rise to clinopyroxenes in the Fuerteventura gabbro xenoliths (Fig. 10), and hypothetical whole rock compositions shown (Fig. 11). *Plag/cpx* and *mt/cpx* values are estimated from the listed mineral/melt partition coefficients. The "Alk. melt" used as a model for trapped melt in Fig. 11 is based on data on mafic, aphyric, alkali basaltic lavas and dykes from Tenerife (Neumann et al. 1999). Where necessary, partition coefficients have been interpolated on the basis of the available data (shown in italics)

	Partition coefficients						Alk. melt
Phases Ref.	Ol/cpx 1, 2	Opx/cpx 2, 3	Cpx/melt 4, 5	Plag/melt 6	Mt/melt 7, 8, 9	Ap/melt 10	 11
Rb	0.5	1.0	0.0047	0.042	*0.004*	0.01	255
Ba	0.3	0.6	0.0006	0.277	*0.0001*	0.74	607
Th	0.05	3.9	0.0056	*0.004*	0.022	0.7	7.79
U	0.3	4.0	0.005	*0.004*	0.02	0.7	1.64
Nb	0.003	0.2	0.0027	*0.004*	0.1	0.001	104
Ta	0.06	0.07	*0.01*	*0.004*	0.1	0.01	8.4
La	0.011	0.014	0.044	0.184	0.003	4.0	69.3
Ce	0.0025	0.014	0.084	0.121	0.003	4.2	140
Pr	*0.003*	0.017	0.124	0.139	*0.0045*	3.4	16
Sr	0.0011	0.018	0.124	1.9	*0.0001*	2.7	1167
Nd	0.003	0.017	0.173	0.121	*0.006*	3.4	55
Zr	0.005	0.08	0.164	*0.0042*	0.1	0.007	338
Hf	0.005	0.192	0.29	*0.004*	0.31	0.01	7.8
Sm	0.003	0.026	0.28	0.139	0.0072	3.1	12.5
Eu	0.003	0.038	0.31	0.088	*0.0065*	2.8	3.44
Ti	0.018	0.40	0.36	*0.001*	1.0	*0.006*	22200
Gd	0.003	0.043	0.34	0.07	0.0055	1.7	9.3
Tb	0.004	0.056	0.36	0.05	*0.006*	2.2	1.34
Dy	0.004	0.071	0.41	0.029	*0.006*	1.8	7.1
Y	0.004	0.091	0.44	0.0315	0.004	3.1	37
Ho	*0.004*	0.091	0.41	*0.022*	0.008	1.7	1.07
Er	0.004	0.116	0.41	0.0181	*0.007*	1.4	2.7
Tm	0.006	0.140	0.41	*0.012*	*0.005*	1.00	0.37
Yb	0.009	0.182	0.41	*0.006*	*0.003*	0.93	2.2
Lu	0.016	0.227	0.43	0.0027	0.023	0.75	0.33

Ol olivine, *cpx* clinopyroxene, *plag* plagioclase, *mt* magnetite, *ap* apatite
1 Eggins et al. (1998), *2* Garrido et al. (2000), *3* Green et al. (2000), *4* Hauri et al. (1994), *5* Foley et al. (1996), *6* Bindeman and Davis (2000), *7* Nielsen et al. (1992), *8* Nielsen et al. (1994), *9* Horn et al. (1994), *10* Ionov et al. (1997), *11* Neumann et al. (1999)

10, 11, 12) represent robust evidence against the possibility that a mantle plume can have affected the area of the Canary Islands during the opening of the central Atlantic Ocean. It has been shown that also the upper mantle beneath the Canary Islands, including the easternmost islands Lanzarote and Fuerteventura, originated as a highly refractory oceanic lithospheric mantle (Neumann et al. 2002; M.M. Abu El-Rus and E.-R. Neumann, unpublished data).

The continental slope off western Morocco south of the Canary Islands is relatively steep. The island Fuerteventura appears to be built partly onto the continental slope (Fig. 2). This means that the true base of the continental slope probably lies west of the bottom of the submarine valley between Fuerteventura and the continental slope, close to the eastern coast of Fuerteventura. This is illustrated in Fig. 13, which represents a simplified profile along the line A–A′ in Fig. 2. In areas with wide transition zones between "normal" continental and oceanic crust, like in the Iberian Abyssal Plain (Fig. 1) and the Red Sea, these transition zones are found seawards of the base of the continental slope. The presence of an old oceanic lower crust and upper mantle beneath Fuerteventura (as well as that beneath the other Canary Islands) implies that the continent–ocean transition in the Canary Islands area must be quite sharp, that is less than the distance between the base of the

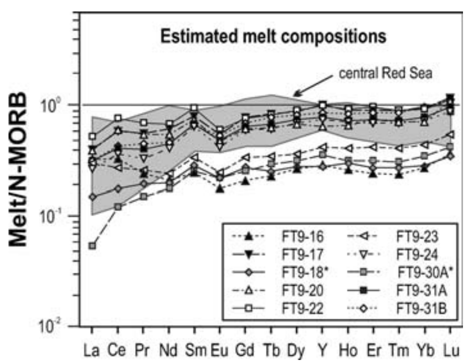

Fig. 10 Estimated REE concentrations in melts that gave rise to gabbroic xenoliths in Fuerteventura, normalized to average N-MORB (Hofmann 1988). The estimates are based on clinopyroxene and orthopyroxene data (this study) and the partitioning of REE between pyroxenes and basaltic melts (cpx/melt: data on Ti–Al-poor cpx from Hill et al. 2000, with adjustment of $Tm_{cpx/melt}$ to 0.76; opx/melt: Green et al. 2000). For comparison are also shown the REE patterns of glasses and crystalline rocks collected along the mid-ocean ridge in the central Red Sea (Altherr et al. 1988)

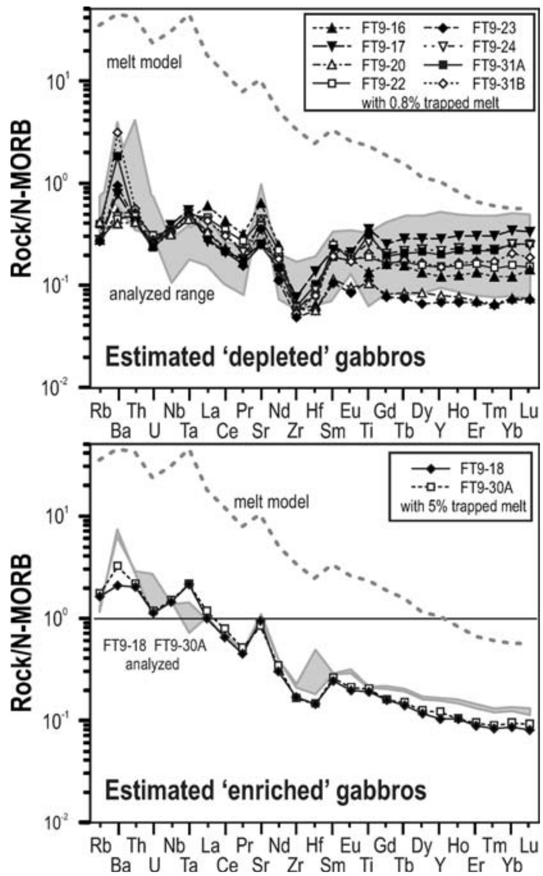

Fig. 11 Observed gabbro compositions compared to estimated ones based on the assumptions that the gabbros represent N-MORB cumulates infiltrated by alkali basaltic Canarian magmas, and that olivine, clinopyroxene, orthopyroxene, and plagioclase belong to the original N-MORB gabbro assemblage, whereas oxide and apatite have formed from the infiltrating melt. We have used the analytical data for clinopyroxene and orthopyroxene (Tables 5 and 7), and estimated the trace element compositions of olivine and plagioclase from clinopyroxene data combined with olivine/clinopyroxene, clinopyroxene/melt, and plagioclase/melt partition coefficients for tholeiitic basaltic systems (Foley et al. 1996; Bindeman and Davis 2000; Garrido et al. 2000; Table 9); trace element compositions of apatite and magnetite have been calculated from apatite/melt and magnetite/melt partition coefficients in alkaline basalts (Ionov et al. 1997; Nielsen et al. 1992, 1994, respectively; Table 9). The proportion of each phase is given by the norm calculations (Table 1)

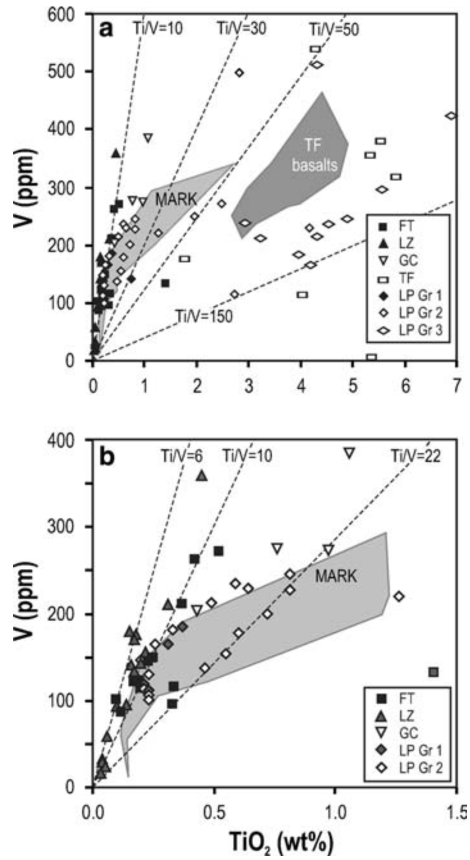

Fig. 12 V–TiO_2 relationships in gabbro xenoliths of different types from the Canary Islands (this study; Schmincke et al. 1998; Neumann et al. 2000), compared to gabbroic rocks from the MARK area along the central MAR (data from Casey 1997) and aphyric basalts from Tenerife (TF basalts; Neumann et al. 1999). *FT* Fuerteventura, *LZ* Lanzarote, *GC* Gran Canaria, *TF* Tenerife, *LP* La Palma. Samples from Fuerteventura, Lanzarote, and La Palma Gr 1 (*filled symbols*) represent N-MORB gabbros infiltrated by very small amounts of enriched melts. Samples from Gran Canaria and La Palma Gr 2 represent N-MORB gabbros infiltrated by significant amounts of enriched melts. Samples from Tenerife and La Palma Gr 3 comprise gabbroic rocks formed from enriched Canary Islands magmas. The Ti/V ratios increase from the N-MORB gabbros least affected by Canary Islands melts (Ti/V≈6) to those that have formed from Canarian magmas (Ti/V≈50). See text for discussion

continental platform and the east coast of Fuerteventura.

The sharp continent–ocean transition found to exist along the eastern Atlantic Ocean in the Morocco-Canary Islands area is significantly different from that further north, where the 80 to 130-km-wide transition zone along the Iberian peninsula is well documented (e.g. Boillot and Winterer 1988; Pinheiro et al. 1996; Whitmarsh and Sawyer 1996; Chian et al. 1999). Also at the base of the Mazagan escarpment, about 100 km west of the coast of Morocco, north of the Canary Islands (Fig. 1), continental crust (consisting of highly deformed, ca. 515 million years old granodioritic gneisses) has been recovered at about 4,000 m water depth by Deep Sea Drilling (DSDP Leg 79, Hole 544A; Kreuzer et al. 1984). This suggests that the continental break-up also in this area is related to strong attenuation of the continental crust, and possibly results in the incorporation of pieces of old continental crust in the newly formed oceanic crust. The reason for the different styles in developing the passive margin along Morocco and Iberian peninsula is so far unknown.

Summary of conclusions

Gabbro xenoliths collected in northern Fuerteventura are very fresh and consist of Ti–Al-poor clinopyroxene + plagioclase ($An_{87–67}$) + olivine ($Fo_{72–86}$) ± orthopyroxene. Our studies of these xenoliths have led to the following observations and conclusions:

1. Clinopyroxene and orthopyroxene are markedly depleted in LREE relative to HREE, but show enrichment factors (normalized to primordial mantle) for the most strongly incompatible elements close to those of the LREE
2. Clinopyroxenes formed from melts with strongly depleted REE patterns, implying that they originally belonged to a highly refractory N-MORB lower crust
3. Whole-rock trace element patterns range from mildly S-shaped (mildly depleted in Pr–Sm relative to both the strongly incompatible elements Rb–La and the HREE) to ones enriched in the most strongly incompatible element, including LREE, relative to HREE
4. The trace element compositions are compatible with the formation of the gabbroic xenoliths as cumulates from N-MORB basaltic magmas and their successive infiltration at various extents ($\leq 1\%$ to $> 5\%$) by enriched alkali basaltic melts
5. Infiltration and enrichment occurred during the Canary Islands magmatic event, possibly by the host lavas that brought the samples to the surface; this result contradicts the claim that a mantle plume was present in the area during the opening of the Atlantic Ocean
6. The trace element compositions of the gabbro xenoliths from Fuerteventura closely resemble those of the most depleted samples from other Canary Islands, implying a uniform degree of partial melting of a uniform mantle source during the first ca. 30 million years of opening of this part of the Atlantic Ocean;
7. The presence of the N-MORB oceanic crust (and mantle) beneath Fuerteventura implies that the continent–ocean transition outside western Morocco must be relatively sharp, in contrast to the 80 to 130-km-wide transition zone along the Iberian peninsula, further north.

Acknowledgements This project was made possible through grants from the Norwegian Research Council (NFR). We are grateful to Muriel Erambert for helping with the microprobe analyses.

References

Abdel-Monem A, Watkins ND, Gast PW (1971) Potassium–argon ages, volcanic stratigraphy, and geomagnetic polarity history of the Canary Islands: Lanzarote, Fuerteventura, Gran Canaria, and La Gomera. Am J Sci 271:490–521

Abdel-Monem A, Watkins ND, Gast PW (1972) Potassium-argon ages, volcanic stratigraphy, and geomagnetic polarity history of the Canary Islands: Tenerife, La Palma, and Hierro. Am J Sci 272:805–825

Ahijado A, Casillas R, Hernández-Pacheco A (2001) The dyke swarms of the Amanya Massif, Fuerteventura, Canary Islands (Spain). J Asian Earth Sci 19:333–345

Altherr R, Henjes-Kunst F, Puchelt H, Baumann A (1988) Volcanic activity in the Red Sea Axial trough—evidence for a large mantle diaper? Tectonophysics 150:121–133

Balogh K, Ahijado A, Casillas R, Fernandez C (1999) Contributions to the chronology of the Basal Complex of Fuerteventura, Canary Islands. J Volcanol Geotherm Res 90:81–101

Bindeman IN, Davis AM (2000) Trace element partitioning between plagioclase and melt: investigation of dopant influence on partition behaviour. Geochim Cosmochim Acta 64:2863–2878

Boillot G, Winterer E (1988) Drilling on the Galicia margin: retrospect and prospect. Proc Ocean Drill Prog Sci Results 103:809–828

Boillot G, Féraud G, Recq M, Girardeau J (1989) Undercrusting by serpentinite beneath rifted margins. Nature 341:523–524

Bonatti E (1985) Punctiform initiation of seafloor spreading in the Red Sea during transition from a continental to an oceanic rift. Nature 316:33–37

Cannat M, Chatin F, Whitechurch H, Ceuleneer G (1997) Gabbroic rocks trapped in the upper mantle at the Mid-Atlantic Ridge. Proc Ocean Drill Prog Sci Results 153:243–264

Carracedo JC, Day S (2002) Canary Islands. Classical geology in Europe, vol 4. Terra Publishing, Harpenden, p 294

Casey JF (1997) Comparison of major and trace-element geochemistry of abyssal peridotites and mafic plutonic rocks with basalt from the MARK Region of the Mid-Atlantic Ridge. Proc Ocean Drill Prog Sci Results 153:181–241

Chian D, Keen C, Reid I, Louden KE (1995) Evolution of nonvolcanic rifted margins: new results from the conjugate margins of the Labrador Sea. Geology 23:589–592

Chian D, Louden KE, Minshull TA, Whitmarsh RB (1999) Deep structure of the ocean-continent transition in the southern Iberian Abyssal Plain from seismic refraction profiles: Ocean Drilling Program (Legs 149 and 173) transect. J Geophys Res 104:7443–7462

Cochran JR (1983) A model for development of Red Sea. Am Assoc Petroleum Geol Bull 67:41–69

Coello J, Cantagrel JM, Hernan F, Fúster JM, Ibarrola E, Ancochea E, Casquet C, Jamond C, Diaz TJR, Cendrero A (1992). Evolution of the eastern volcanic ridge of the Canary Islands based on new K–Ar data. J Volcanol Geotherm Res 53:251–274

Coogan LA, Kempton PD, Saunders AD, Norry MJ (2000) Melt aggregation within the crust beneath the Mid-Atlantic Ridge: evidence from plagioclase and clinopyroxene major and trace element compositions. Earth Planet Sci Lett 176:245–257

Cornen G, Beslier M-O, Girardeau J (1996a) Petrologic characteristics of the ultramafic rocks from the ocean/continent transition in the Iberia Abyssal Plain. Proc Ocean Drill Prog Sci Results 149:377–395

Cornen G, Beslier M-O, Girardeau J (1996b) Petrology of the mafic rocks cored in the Iberia Abyssal Plain. Proc Ocean Drill Prog Sci Results 149:449–469

Cortesogno L, Gaggero L, Zanetti A (2000) Rare earth and trace elements in igneous and high-temperature metamorphic minerals of oceanic gabbros (MARK area, Mid-Atlantic Ridge). Contrib Mineral Petrol 139:373–393

Eggins SM, Rudnick RL, McDonough WF (1998) The composition of peridotites and their minerals; a laser-ablation ICP-MS study. Earth Planet Sci Lett 154:53–71

Ernst RE, Buchan KL (1997) Giant radiating dyke swarms; their use in identifying pre-Mesozoic large igneous provinces and mantle plumes. In: Mahoney JJ, Coffin MF (eds) Large igneous provinces; continental, oceanic, and planetary flood volcanism. Geophys Monogr 100:297–333

Foley SF, Jackson BJ, Greenough JD, Jenner GA (1996) Trace element partition coefficients for clinopyroxene and phlogopite in an alkaline lamprophyre from Newfoundland by LAM-ICP-MS. Geochim Cosmochim Acta 60:629–638

Fúster JM, Cendrero A, Gastesi P, Ibarrola E, Lopez Ruiz J (1968) Geología y volcanología de las isles Canarias—Fuerteventura. Instituto "Lucas Mallada", Consejo Superior de Investigaciones Científicas, Madrid, p 239

Gaggero L, Cortesogno L (1997) Data report: Metamorphic mineralogy of Leg 153 gabbros. Proc Ocean Drill Prog Sci Results 153:531–546

Garrido CJ, Bodinier JL, Alard O (2000) Incompatible trace element partitioning and residence in anhydrous spinel peridotites and websterites from Ronda orogenic peridotite. Earth Planet Sci Lett 181:341–358

Green TH, Blundy J, Adam J, Yaxley GM (2000) SIMS determinatiopn of trace element partition coefficients between garnet, clinopyroxene and basaltic liquids at 1–7.5 GPa and 1080-1200°C. Lithos 53:165–187

Hannigan RE, Basu AR, Teichmann F (2001) Mantle reservoir geochemistry from statistical analysis of ICP-MS trace element data of equatorial mid-Atlantic MORB glasses. Chem Geol 175:397–428

Hauri EH, Wagner TP, Grove TL (1994) Experimental and natural partitioning of Th, U, Pb and other trace elements between garnet, clinopyroxene and basaltic melts. Chem Geol 117:149–166

Hill E, Wood BJ, Blundy JD (2000) The effect of Ca Tschermaks component on trace element partitioning between clinopyroxene and silicate melt. Lithos 53:203–215

Hoernle K (1998) Geochemistry of Jurassic oceanic crust beneath Gran Canaria (Canary Islands): implications for crustal recycling and assimilation. J Petrol 39:859–880

Hofmann AW (1988) Chemical differentiation of the Earth: the relationship between mantle, continental crust, and oceanic crust. Earth Planet Sci Lett 90:297–314

Horn I, Foley SF, Jackson SE, Janner GA (1994) Experimentally determined partitioning of high field strength- and selected transition elements between spinel and basaltic melt. Chem Geol 117:193–218

Ionov DA, Griffin WL, O'Reilly SY (1997) Volatile-bearing minerals and lithophile trace elements in the upper mantle. Chem Geol 141:153–184

Janney PE, Castello PR (2001) Geochemistry of the oldest Atlantic oceanic crust suggests mantle plume involvement in the early history of the central Atlantic Ocean. Earth Planet Sci Lett 192:291–302

Komor SC, Grove TL, Hebert R (1990) Abyssal peridotites from ODP Hole 670A (21°10′N, 45°02′W); residues of mantle melting exposed by non-constructive axial divergence. Proc Ocean Drill Prog Sci Results 106/109:85–101

Kreuzer H, Müller P, Wissmann G, Reinecke T (1984) Petrography and K–Ar dating of the Mazagan granodiorite. Deep Sea Drill Proj Leg 79, Holes 544A and 547B:543–549

Le Bas MJ, Rex DC, Stillman CJ (1986) The early magmatic chronology of Fuerteventura. Geol Mag 123:287–298

Martinez F, Cochran JR (1988) Structure and tectonics of the northern Red Sea; catching a continental margin between rifting and drifting. In: Bonatti E (ed) Zabargad Island and the Red Sea Rift. Tectonophysics 150:1–32

McDonough WF, Sun S-s (1995) The composition of the Earth. Chem Geol 120:223–253

McHone JG (2000) Non-plume magmatism and rifting during the opening of the central Atlantic Ocean. Tectonophysics 316:287–296

Morgan JV, Barton PJ (1990) A geophysical study of the Hatton Bank volcanic margin; a summary of the results from a combined seismic, gravity and magnetic experiment. In: Leven JH, Finlayson DM, Wright C, Dooley JC, Kennett BLN (eds) Seismic probing of continents and their margins. Tectonophysics 173:517–526

Morgan JV, Barton PJ, White RS (1989) The Hatton Bank continental margin; III, Structure from wide-angle OBS and multichannel seismic refraction profiles. Geophys J R Astro Soc 98:367–384

Müller RD, Roest WR, Royer JY, Gahagan LM, Sclater JG (1997) Digital isochrons of the world's ocean floor. J Geophys Res 102:3211–3214

Mutter JC, Zehnder CM (1988) Deep crustal structure and magmatic processes; the inception of seafloor spreading in the Norwegian-Greenland Sea. Geol Soc Spec Publ 39:35–48

Neumann E-R, Wulff-Pedersen E, Simonsen SL, Pearson NJ, Mitjavila J, Martí J (1999) Evidence for fractional crystallization of periodically refilled magma chambers in Tenerife, Canary Islands. J Petrol 40:1089–1123

Neumann E-R, Sørensen V, Simonsen SL, Johnsen K (2000) Gabbroic xenoliths from La Palma, Tenerife and Lanzarote, Canary Islands: evidence for reactions between Canary Islands melts and old oceanic crust. J Volcanol Geotherm Res 103:313–342

Neumann E-R, Griffin WL, Normann JP, O'Reilly SY (2004) The evolution of the upper mantle beneath the Canary Islands: information from trace elements and Sr isotope ratios in minerals in mantle xenoliths. J Petrol 45:2573–2612

Nielsen RL, Gallahan WE, Newberger F (1992) Experimentally determined mineral-melt partition coefficients for Sc, Y and REE for olivine, orthopyroxene, pigeonite, magnetite and ilmenite. Contrib Mineral Petrol 110:488–499

Nielsen RL, Forsythe LM, Gallahan WE, Fisk MR (1994) Major- and trace-element magnetite-melt equilibria. Chem Geol 117:167–191

Niida K (1997) Mineralogy of MARK peridotites: replacement through magma channelling examined from Hole 920D, MARK area. Proc Ocean Drill Prog Sci Results 153:265–275

Pérez-Gussinyé M, Reston TJ (2001) Rheological evolution during extension at nonvolcanic rifted margins: onset of serpentinization and development of detachments leading to continental breakup. J Geophys Res 106:3961–3975

Pinheiro LM, Wilson RCL, Pena dos Reis R, Whitmarsh RB, Ribeiro A (1996) The western Iberia margin: a geophysical and geological overview. Proc Ocean Drill Prog Sci Results 149:3–23

Reid ID (1994) Crustal structure of a nonvolcanic rifted margin east of Newfoundland. J Geophys Res 99:15161–15180

Roeser HA (1975) A detailed magnetic survey of the southern Red Sea. Geol Jahrb 13:131–153

Roest WR, Dañobeitia JJ, Verhoef J, Collette BJ (1992) Magnetic anomalies in the Canary Basin and the Mesozoic evolution of the central North Atlantic. Mar Geophys Res 14:1–24

Ross K, Elthon D (1997) Cumulus and postcumulus crystallization in the oceanic crust: major- and trace-element geochemistry of Leg 153 gabbroic rocks. Proc Ocean Drill Prog, Sci Results 153:333–350

Schilling J-G (1973) Iceland Mantle Plume: geochemical study of Reykjanes Ridge. Nature 242:565–571

Schilling J-G, Zajac M, Evans R, Johnston T, White W, Devine JD, Kingsley R (1983) Petrologic and geochemical variations along the Mid-Atlantic Ridge from 29°N to 73°N. Am J Sci 238:510–586

Schmincke H-U (1982) Volcanic and Chemical evolution of the Canary Islands. In: von Rad U, Hinz K, Sarnthein M, Seibold E (eds) Geology of the northwest African continental margin. Springer, Berlin Heidelberg New York, pp 274–306

Schmincke H-U, Klügel A, Hansteen TH, Hoernle K, van den Bogaard P (1998) Samples from the Jurassic crust beneath Gran Canaria, La Palma and Lanzarote (Canary Islands). Earth Planet Sci Lett 163:343–360

Seifert KE, Brunotte DA (1996) Geochemistry of serpentinized mantle peridotite from Site 897 in the Iberia Abyssal Plain. Proc Ocean Drill Prog, Sci Results 149:413–424

Seifert KE, Gibson I, Weis D, Brunotte DA (1996) Geochemistry of metamorphosed cumulate gabbros from Hole 900A, Iberia Abyssal Plain. Proc Ocean Drill Prog, Sci Results 149:471–488

Seifert KE, Chang C-W, Brunotte DA (1997) Evidence from Ocean Drilling Program Leg 149 mafic igneous rocks for oceanic crust in the Iberia Abyssal Plain ocean-continent transition zone. J Geophys Res 102:7915–7928

Shervais JW (1982) Ti-V plots and the petrogenesis of modern and ophiolitic lavas. Earth Planet Sci Lett 59:101–118

Skelton ADL, Valley JW (2000) The relative timing of serpentinization and mantle exhumation at the ocean-continent transition, Iberia: constraints from oxygen isotopes. Earth Planet Sci Lett 178:327–338

Stephens CJ (1997) Heterogeneity of oceanic peridotites from the western canyon wall at MARK: results from Site 920. Proc Ocean Drill Prog, Sci Results 153:285–303

Stillman CJ (1987) A Canary Islands dyke swarm: implications for the formation of oceanic islands by extensional fissural volcanism. In: Halls JM, Fahrig WF (eds) Mafic dyke swarms. Geol Ass Canada, Spec Pap 34:243–255

Stillman CJ, Fúster JM, Bennell-Baker MJ, Muñoz M, Smewing JD, Sagredo J (1975) Basal complex of Fuerteventura, (Canary Islands) is an oceanic intrusive complex with rift-system affinities. Nature 257:469–471

Sun S-S, McDonough WF (1989) Chemical and isotopic systematics of oceanic basalts: implications for mantle composition and processes. Geol Soc Spec Publ 42:313–345

Tiepolo M, Bottazzi P, Palenzona M, Vannucci R (2003) A laser probe coupled with ICP – double-focusing sector-field mass spectrometer for in situ analysis of geological samples and U-Pb dating of zircon. Can Mineral 41:259–272

Verhoef J, Collette BJ, Da˜nobeitia JJ, Roeser HA, Roest WR (1991) Magnetic anomalies off West-Africa (20-38°N). Marine Geophys Res 13:81–103

Watts AB (1994) Crustal structure, gravity anomalies and flexure of the lithosphere in the vicinity of the Canary Islands. Geophys J Internat 119:648–666

Whitmarsh RB, Sawyer DS (1996) The ocean/continent transition beneath the Iberia Abyssal Plain and continental-rifting to seafloor spreading processes. Proc Ocean Drill Prog, Sci Results 149:713–733

Wilson M, Guiraud R (1998) Late Permian to Recent magmatic activity on the African-Arabian margin of Tethys. Geol Soc Lond Spec Publ 132:231–263